Power Loss Investigation of Pavement Materials in Roadway Inductive Charging System

Zilong Zheng
Dept. of Electrical and Computer Engineering
Drexel University
Philadelphia, USA
zz529@drexel.edu

Yao Wang
Dept. of Electrical and Computer Engineering
Drexel University
Philadelphia, USA
yw696@dragons.drexel.edu

Xiao Chen
Dept. of Civil and Environmental Engineering
Rutgers University
Piscataway, USA
xc299@scarletmail.rutgers.edu

Shuyan Zhao
Dept. of Electrical and Computer Engineering
Drexel University
Philadelphia, USA
sz568@drexel.edu

Shervin Salehi Rad
Dept. of Electrical and Computer Engineering
Drexel University
Philadelphia, USA
ss5485@drexel.edu

Hua Zhang
Dept. of Electrical and Computer Engineering
Rowan University
Glassboro, USA
zhangh@rowan.edu

Hao Wang
Dept. of Civil and Environmental Engineering
Rutgers University
Piscataway, USA
hw261@soe.rutgers.edu

Fei Lu
Dept. of Electrical and Computer Engineering
Drexel University
Philadelphia, USA
fl345@drexel.edu

2024 IEEE Applied Power Electronics Conference and Exposition (APEC) | 979-8-3503-1664-3/24/$31.00 ©2024 IEEE | DOI: 10.1109/APEC48139.2024.10509424

***Abstract*—Inductive power transfer (IPT) technology has emerged as a promising wireless charging solution for electric vehicles. However, the application of IPT often overlooked the interaction between an IPT system and different pavement materials. When the transmitter coil is embedded inside a pavement material, the power loss is different due to the properties of different pavement materials (asphalt or concrete) as the transfer medium. This paper presents an experimental investigation into the power loss of different asphalt and concrete materials under varying magnetic flux intensity *B* and frequency *f*. A total of seven categories of pavement materials are tested, including 4 concrete materials and 3 asphalt materials. A solenoid coil is employed to generate a uniformly distributed magnetic field up to 5.36mT, and test frequency *f* of 80kHz, 85kHz, and 90kHz are chosen following the SAE-2954 standard. Experimental results reveal that at each frequency *f*, there is an exponential increase in power loss in pavement materials as *B* increases, with that the concrete materials demonstrating overall higher power loss compared to the asphalt materials. For further analysis, an IPT system is established to compare the impact of different pavement materials.**

Keywords—Inductive power transfer (IPT), power loss, road pavement material, wireless power transfer (WPT)

I. Introduction

As the development of wireless power transfer (WPT) technology for electric vehicles (EVs) becomes more and more mature, there are more dedicated research focusing on how to utilize WPT technology to benefit the implementation of the intelligent transportation systems (ITS), smart grids, and various Internet to Vehicle (ToV) applications [1]-[2]. Inductive power transfer (IPT), one of the most widely used WPT technology, offers a promising solution to provide a smarter, more flexible, and more convenient charging solution [3]-[4]. Currently, there are two main methods of recharging EVs wirelessly. One is stationery wireless charging (SWC). The other method is to charge an EV while it is in motion, which usually referred to as dynamic wireless charging (DWC). In DWC, EVs can use a smaller onboard battery pack which reduces the weight and cost of EVs [5]-[7]. Both stationary and dynamic charging concepts have been proposed, in which the transmission side of the charging pad is embedded in road pavements, resulting undisrupted motion of the vehicles. The charging process is established after a vehicle approaches a designated spot triggering the charging process. The onboard batteries of an EV can be charged without a physical connection. This wireless charging process removes the charging cables and human involvement in the EV charging process resulting in a safer, faster, and more robust energy transfer solution to meet the need of ITS [8]-[9].

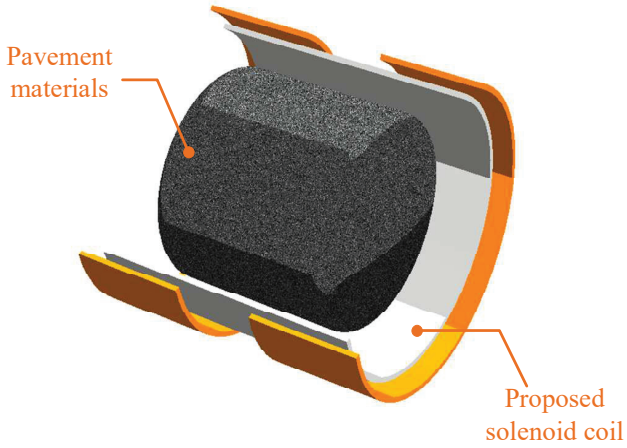

Figure 1: Conceptual structure of the solenoid coils

In practical applicatoins, the transmitter side of an IPT system is embedded inside the pavement materials. During the charging process, various pavement materials, such as asphalt and concrete, act as the transfer medium between transmitter and receiver sides. These materials can cause extra power loss and impact the overall efficiency of the IPT system [10]-[12]. Analyzing and modeling power loss in various pavement materials from both electromagnetics and physics perspectives is inherently complex due to the diverse composition of pavements. Therefore, an experimental investigation was designed to observe and understand this power loss phenomenon. In this paper, a resonant LCR circuit is used to generate a sinusoidal current to excite a solenoid coil, aiming at an evenly distributed field.

Fig. 7. Shows three hot mix asphalt samples, named R1, HPOT, and SMA and the 4 cement concrete material samples named Cement1, Cement2, Cment3, and Cement4. are constructed in a cylinder shape and tested inside of a solenoid coil as shown in Fig. 1.

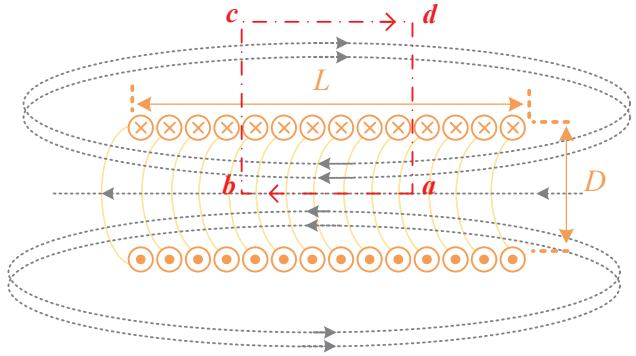

Figure 2: Magnetic flux distribution of a solenoid coil.

There are three innovative contributions in this paper. 1)The increase of power loss induced by both concrete and asphalt materials are recorded and compared under different frequency f and the magnetic flux intensity B. 2) Experimental analysis revealed that the power density D_p (W/L) for all the pavement materials have a noticeable increase in power loss when they are compared to the situation where only air acts as a transfer medium. 3) The power loss density difference among the concrete and asphalt materials.

II. Design of an Evently Distrubuted Magnetic Field

A. Theoretical Analysis of magnetic Field Generated by A Solenoid Coil

In a practical IPT system, the distribution of the magnetic field in space is not uniform, which presents challenges in studying the correlation between power loss in pavement materials and the magnetic flux intensity B. However, this paper addresses this issue by employing solenoid coils. These coils can produce a consistent magnetic field within their internal space, especially when the length L is significantly greater than the diameter D. This characteristic allows for a more controlled and precise investigation of the relationship between power loss in pavement materials and the magnetic flux intensity.

Fig. 2. Shows the magnetic flux distribution of a solenoid coil. According to Ampere's Law, the integral of B along closed loop l_{abcd} is given by (1). μ_0 is the magnetic permeability and N is the number of turns enclosed by the loop l_{abcd}. Equ. (1) is further expressed as (2). When the length L is much longer than the diameter D, the inside magnetic field is strong and uniform, which means B_{bc}, B_{cd}, and B_{da} are negligible compared to B_{ab}. Therefore, the internal B is calculated by (3) and (4).

$$\int_{l_{abcd}} B \cdot dl = \mu_0 iN, (\mu_0 = 4\pi \times 10^{-7} H/m) \quad (1)$$

$$\int_{l_{abcd}} Bdl = \int_{l_{ab}} B_{ab}dl + \int_{l_{bc}} B_{bc}dl + \int_{l_{cd}} B_{cd}dl + \int_{l_{da}} B_{da}dl \quad (2)$$

$$\int_{l_{abcd}} B \cdot dl = \int_{l_{ab}} B_{ab} \cdot dl = \mu_0 iN \quad (3)$$

$$B = B_{ab} = \frac{\mu_0 iN}{l_{ab}} = \frac{4\pi \times 10^{-7} \times 16 \times 168}{0.596} = 5.67mT \quad (4)$$

B. Solenoid Coil Implementation and Magnetic Field Simulation

Fig. 3(a) demonstrates the implemented solenoid coil. The 3000-strand 0.04mm AWG 46 Litz wire is used to construct a

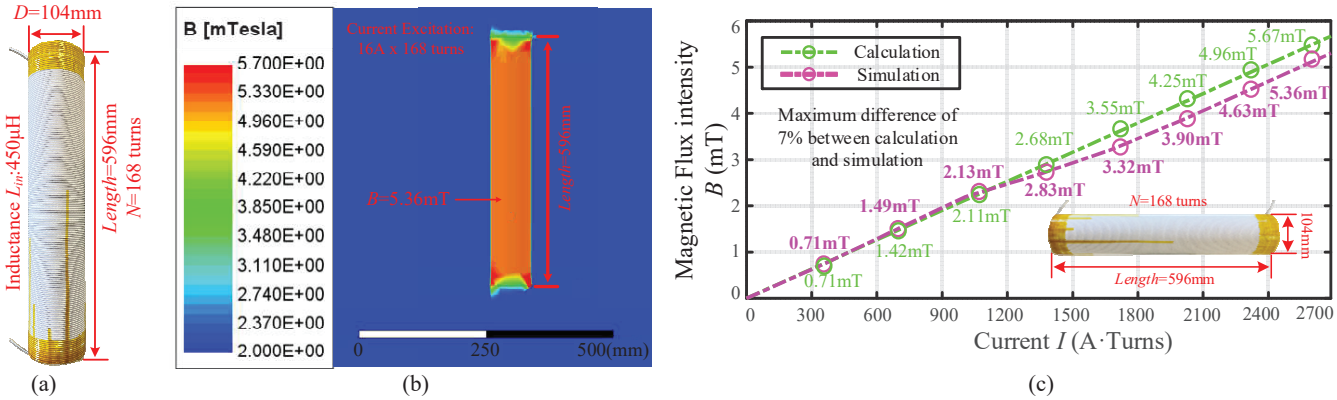

Figure 3: (a) Constructed solenoid coil; (b) B-field simulation; (c) Calculated and simulated magnetic intensity B.

coil with 168 turns, a length L of 596mm, and a diameter D of 104mm, achieving an inductance L_{in}=450μH. Each of the pavement materials is placed inside the solenoid coil individually for testing.

Fig. 3(b) shows simulated magnetic field generated with a current excitation of i=16A and coil turns of N=168. The internal magnetic flux intensity B is almost spatially even.

Fig. 3(c) compares simulated and calculated B generated at different excitations, which shows high consistency, validating the proposed design of a uniform magnetic field. Particularly, with i=16A and N=168, the simulated B is 5.36mT, which only has a 7% difference from the calculated 5.67mT.

III. Experimental Test on Pavement Maerials

A. Pavement Material Test Platform

An experimental platform is shown in Fig. 4. The inverter is built based on silicon carbide (SiC) MOSFET C2M0040120D. The *LCR* resonant circuit produces a sinusoidal current. The equivalent circuit is shown in Fig. 5. The parasitic resistance of the inductor and capacitor is represented by R_{LC} and R_M represents the equivalent resistance of pavement material. The experiment was conducted using the operating frequency of 80kHz, 85kHz, and 90kHz. The current ranges from 0 to 16A. The system total loss P_{tot} includes the inverter loss P_{inv}, passive loss P_{LC} and pavement loss P_M. When the circuit works in air, the power loss is represented by P_{air}, which only includes P_{inv} and P_{LC}. The power loss relationship is represented by (5).

All cement concretes have a volume of V_c= 1570mL and all the asphalts have a volume of V_a= 943mL. The system power loss of 3 hot mix asphalt materials P_{R1}, P_{HPOT}, and P_{SMA}, and 4 cement concrete materials P_{C1}, P_{C2}, P_{C3}, and P_{C4} are recorded using an experiment setup in Fig.4. Power density D_p (W/L) is introduced to assess power loss property of materials as defined in (6).

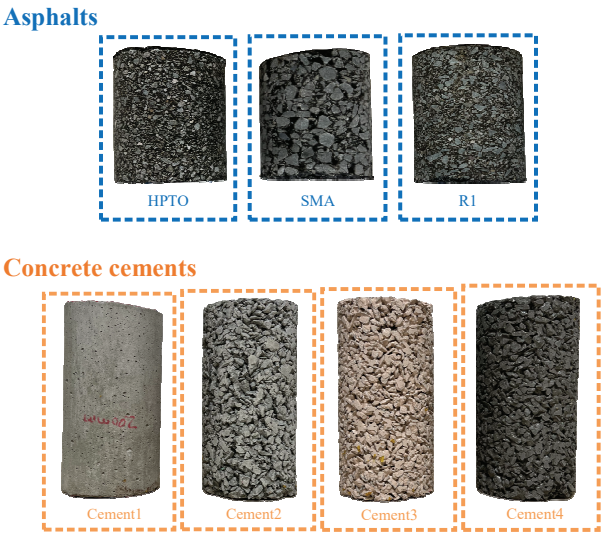

Figure 7: Asphalts and Concrete Pavements

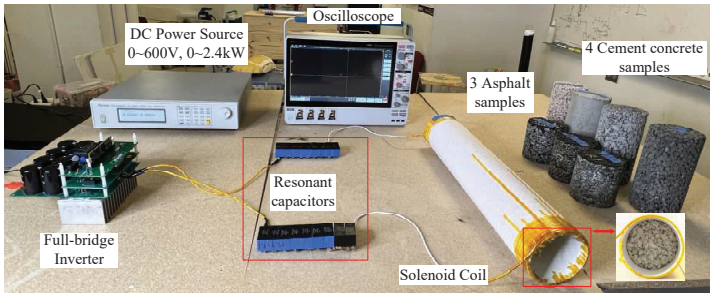

Figure 4: Experiment test platform for pavement materials.

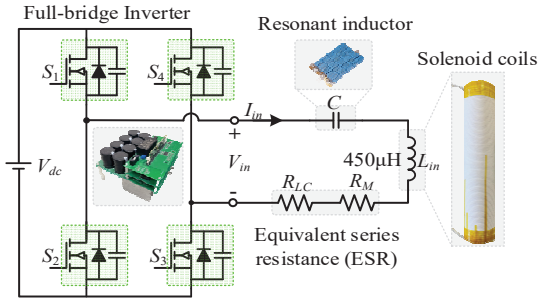

Figure 5: Equivalent RLC resonant circuit.

B. System Power Loss for the Concrete and Asphalt

Figs. 6(a), (b), and (c) demonstrate the power loss density of different pavement materials versus their current excitations (magnetic flux intensity B) under three frequencies of 80kHz, 85kHz, and 90kHz. It shows that the cement concrete materials (Cement1- Cement4) tend to have much higher power loss than the asphalt materials (HPTO, SMA, and R1). Particularly, the asphalt R1 has little impact on the increasing of the system

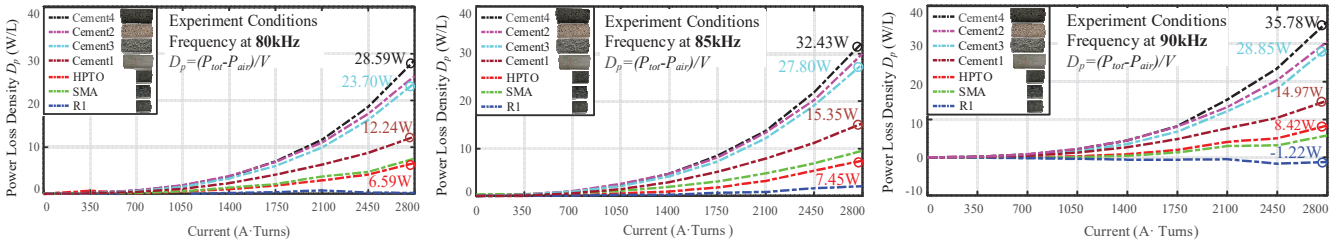

(a) (b) (c)

Figure 6: (a) f=80kHz B-field intensity. (b) f=85kHz B-field intensity. (c) f=90kHz B-field intensity.

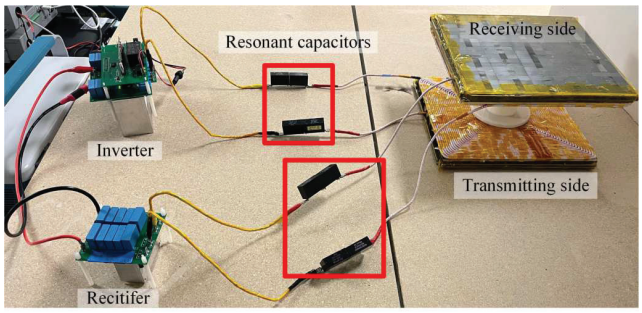

(a)

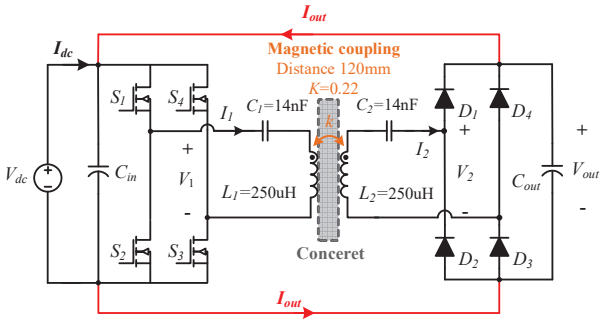

(b)

Figure 8: (a) A 4 kW IPT prototype. (b) Series-series IPT circuit.

power loss, while the other pavement materials tend to exponentially increase the power loss with the magnetic flux intensity B. Furthermore, with a given magnetic field B, higher frequency tends to cause higher loss. The results are useful to evaluate pavement materials.

C. Inductive Power Transfer Setup

Fig. 8(a) shows the implemented series-series IPT prototype, and Fig. 8(b) demonstrates the equivalent IPT circuit. The transmitter and receiver coils, L_1 and L_2 are constructed by using 800-strand 0.1mm Litz wire with the inductance of L_1=L_2=250μH. The distance between the transmitter and receiver is 120mm with a coupling coefficient of k=0.22. The input and output DC voltage is set at V_{dc}=400V and a switching frequency of 85kHz is achieved. When working in the air, the system achieves a power of 4kW with 97.5% dc-dc efficiency and a total power loss of 107.3W. The next step is to test the impact of the 7 pavement materials on the established SS IPT system at different power levels.

IV. Conclusion and Future Work

This digest investigates the power loss on pavement materials for a roadway IPT system. Power loss density D_{R1}, D_{HPTO}, D_{SMA}, D_{C1}, D_{C2}, D_{C3}, and D_{C4} of 7 pavement materials are measured at different frequencies and magnetic field intensities. Experimental results show that the system power loss rises as the magnetic field intensity B and frequency f increase and the cement concrete materials tend to generate higher power loss than asphalt materials. Future work will further investigate the impact of pavement materials on a practical IPT system's efficiency and provide guidance to select the optimal pavement material for various applications.

References

[1] I. Ahmed, M. Rehan, A. Basit, M. Tufail and K. -S. Hong, "A Dynamic Optimal Scheduling Strategy for Multi-Charging Scenarios of Plug-in-Electric Vehicles Over a Smart Grid," in IEEE Access, vol. 11, pp. 28992-29008, 2023, doi: 10.1109/ACCESS.2023.3258859. J. Clerk Maxwell, A Treatise on Electricity and Magnetism, 3rd ed., vol. 2. Oxford: Clarendon, 1892, pp.68–73.

[2] I. S. Jacobs and C. P. Bean, "Fine particles, thin films and exchange anisotropy," in Magnetism, vol. III, G. T. Rado and H. Suhl, Eds. New York: Academic, 1963, pp. 271–350.

[3] N. Liu et al., "A Heuristic Operation Strategy for Commercial Building Microgrids Containing EVs and PV System," *IEEE Trans. Ind. Electron*., vol. 62, no. 4, pp. 2560-2570, April 2015.

[4] C. -H. Ou, H. Liang and W. Zhuang, "Investigating Wireless Charging and Mobility of Electric Vehicles on Electricity Market," *IEEE Trans. Ind. Electron*., vol. 62, no. 5, pp. 3123-3133, May 2015.

[5] Y. Shanmugam et al., "A Systematic Review of Dynamic Wireless Charging System for Electric Transportation," *IEEE Access*, vol. 10, pp. 133617-133642, 2022

[6] A. C. Bagchi, A. Kamineni, R. A. Zane and R. Carlson, "Review and Comparative Analysis of Topologies and Control Methods in Dynamic Wireless Charging of Electric Vehicles," in IEEE Journal of Emerging and Selected Topics in Power Electronics, vol. 9, no. 4, pp. 4947-4962, Aug. 2021, doi: 10.1109/JESTPE.2021.3058968.

[7] A. Zakerian, S. Vaez-Zadeh and A. Babaki, "A Dynamic WPT System With High Efficiency and High Power Factor for Electric Vehicles," in IEEE Transactions on Power Electronics, vol. 35, no. 7, pp. 6732-6740, July 2020, doi: 10.1109/TPEL.2019.2957294.

[8] A. Mahesh, B. Chokkalingam and L. Mihet-Popa, "Inductive Wireless Power Transfer Charging for Electric Vehicles–A Review," in IEEE Access, vol. 9, pp. 137667-137713, 2021, doi: 10.1109/ACCESS.2021.3116678.

[9] C. C. Mi, G. Buja, S. Y. Choi and C. T. Rim, "Modern Advances in Wireless Power Transfer Systems for Roadway Powered Electric Vehicles," in IEEE Transactions on Industrial Electronics, vol. 63, no. 10, pp. 6533-6545, Oct. 2016, doi: 10.1109/TIE.2016.2574993.

[10] A. Ahmad, M. S. Alam and R. Chabaan, "A Comprehensive Review of Wireless Charging Technologies for Electric Vehicles," in IEEE Transactions on Transportation Electrification, vol. 4, no. 1, pp. 38-63, March 2018, doi: 10.1109/TTE.2017.2771619.

[11] F. Li, X. Sun, S. Zhou, Y. Chen, Z. Hao and Z. Yang, "Infrastructure Material Magnetization Impact Assessment of Wireless Power Transfer Pavement Based on Resonant Inductive Coupling," *IEEE Trans. Intell. Transp. Syst.*, vol. 23, no. 11, pp. 22400-22408, Nov. 2022.

[12] A. Beeldens, P. Hauspie, and H. Perik, "Inductive charging through concrete roads: A Belgian case study and application," in *Proc. 1st Eur. Road Infrastruct. Congr.*, Leeds, U.K., 2016, pp. 1–10.

[13] R. Tavakoli et al., "Magnetizable concrete composite materials for road-embedded wireless power transfer pads," *2017 IEEE Energy Conversion Congress and Exposition (ECCE)*, Cincinnati, OH, USA, 2017, pp. 4041-404.